Numerical Error in Weighting Function-Based Unsteady Friction Models for Pipe Transients

By John Vítkovský[1], Mark Stephens[2], Anton Bergant[3],

Angus Simpson[4], M. ASCE., and Martin Lambert[5]

CE Database Keywords

Friction; Pipes; Transients; Unsteady Flow; Numerical Analysis; Error Analysis

---

[1] Graduate Hydrologist, Water Assessment Group, Department of Natural Resources and Mines, Indooroopilly QLD 4068, Australia. Email: john.vitkovsky@nrm.qld.gov.au

[2] PhD Candidate, Centre for Applied Modelling in Water Engineering, School of Civil and Environmental Engineering, University of Adelaide, Adelaide SA 5005, Australia. Email: mstephen@civeng.adelaide.edu.au

[3] Head, Research, Instrumentation and Control Engineering Department, Litostroj E.I. d.o.o., 1000 Ljubljana, Slovenia. Email: anton.bergant@litostroj-ei.si

[4] Head, Associate Professor, Centre for Applied Modelling in Water Engineering, School of Civil and Environmental Engineering, University of Adelaide, Adelaide SA 5005, Australia. (Corresponding author). Tel: +61 8 8303 5874; Fax: +61 8 8303 4359; Email: asimpson@civeng.adelaide.edu.au

[5] Associate Professor, Centre for Applied Modelling in Water Engineering, School of Civil and Environmental Engineering, University of Adelaide, Adelaide SA 5005, Australia. Email: mlambert@civeng.adelaide.edu.au

Abstract

The accurate simulation of pressure transients in pipelines and pipe networks is becoming evermore important in water engineering. Applications such as inverse transient analysis for condition assessment, leak detection and pipe roughness calibration require accurate modelling of transients for longer simulation periods that, in many situations, requires improved modelling of unsteady frictional behaviour. In addition, the numerical algorithm used for unsteady friction should be highly efficient, as inverse analysis requires the transient model to be run many times. A popular model of unsteady friction that is applicable to a short-duration transient event type is the weighting function-based type, as first derived by Zielke (1968). Approximation of the weighting function with a sum of exponential terms allows for a considerable increase in computation speed using recursive algorithms. A neglected topic in the application of such models is evaluation of numerical error. This paper presents a discussion and quantification of the numerical errors that occur when using weighting function-based models for the simulation of unsteady friction in pipe transients. Comparisons of numerical error arising from approximations are made in the Fourier domain where exact solutions can be determined. Additionally, the relative importance of error in unsteady friction modelling and unsteady friction itself in the context of general simulation is discussed.

Introduction

Slightly compressible unsteady pipe flow can be described by two equations that may be derived from the Reynolds transport theorem (Wylie and Streeter 1993). The conservation of mass for unsteady pipe liquid flow is represented by

$$\frac{\partial H}{\partial t} + V\frac{\partial H}{\partial x} - V\sin\theta + \frac{a^2}{g}\frac{\partial V}{\partial x} = 0 \qquad (1)$$

where H = head, V = average velocity, a = wave speed, g = gravitational acceleration, θ = inclination angle of the pipeline to the horizontal, t = time and x = distance. The conservation of linear-momentum for unsteady pipe liquid flow is represented by

$$\frac{\partial H}{\partial x} + \frac{1}{g}\frac{\partial V}{\partial t} + \frac{V}{g}\frac{\partial V}{\partial x} + h_{fS} + h_{fU} = 0 \qquad (2)$$

where h_{fS} and h_{fU} are the quasi-steady and unsteady components of the total unsteady head loss per unit length. Eqs. 1 and 2 are two non-linear hyperbolic partial differential equations that are typically solved using the method of characteristics (MOC). The convective acceleration terms ($V.\partial H/\partial x$ and $V/g.\partial V/\partial x$) and the slope term ($V\sin\theta$) are typically small for low Mach number flows and hence are neglected in the following analysis. The term h_{fS} in Eq. 2 is given by the Darcy-Weisbach relationship as $h_{fS} = fV|V|/2gD$ where D = pipe diameter and f = steady-state Darcy-Weisbach friction factor. This paper is concerned with the accurate and efficient calculation of the term h_{fU} in Eq. 2.

Background

Zielke (1968) developed an analytical solution for the unsteady shear stress in laminar flows in the Laplace domain. The implementation incorporated a two-dimensional axi-symmetric laminar flow solution that had the desirable property that it could easily be applied to the one-dimensional unsteady pipe flow equations and, in particular, in the widely used MOC. The Zielke (1968) solution for the unsteady head loss per unit length, h_f, is

$$h_{fU}(t)_{true} = \frac{16\nu}{gD^2}\left(\frac{\partial V}{\partial t} * W\right)(t) \qquad (3)$$

where ν = kinematic viscosity, W = weighting function and $*$ represents convolution. The unsteady head loss term is a convolution of past fluid accelerations with a weighting function. Herein, this type of model is referred to as a weighting function-based (WFB) model. Zielke (1968) determined a weighting function applicable to laminar flows. Weighting functions exist for smooth-pipe turbulent flows (Vardy and Brown 1995, 1996, 2003; Zarzycki 1997, 2000) and rough-pipe turbulent flows (Vardy and Brown, 2004a).

The WFB model takes into account the two-dimensional behaviour of the velocity profile that results in frequency-dependent attenuation and slight frequency-dependent dispersion of the transient. Previous research has demonstrated the accuracy of WFB models for unsteady friction simulation. Vardy and Hwang (1991) showed good matches between a two-dimensional shell model of transient laminar flow and the Zielke weighting function. Ghidaoui and Mansour (2002) showed that the Vardy-Brown weighting function produced good matches with the quasi-2D model of Pezzinga (1999) for smooth pipe turbulent flow and with experimental data. It should be noted that WFB models give good agreement for flows with strong transients, but less agreement when applied to continuous acceleration or deceleration in turbulent flows.

Numerical Computation of h_{fU} in Weighting Function-Based Models

A number of different approaches have been proposed to evaluate the convolution in Eq. 3. Zielke (1968) implemented the weighting function for laminar flow as a full convolution in the MOC grid, and this implementation is herein called the full convolution method. The convolution integral was approximated using the rectangular rule and the acceleration term was approximated using a centred finite difference as

$$h_{fU}(t)_{app} = \frac{16\nu}{gD^2} \sum_{j=1,3,5,\ldots}^{M} \left[V(t - j\Delta t + \Delta t) - V(t - j\Delta t - \Delta t)\right] W(j\Delta t) \tag{4}$$

where $M = t/\Delta t - 1$. This implementation is very computationally intensive requiring a convolution at every point in the MOC grid in both space and time. Additionally, as the simulation time increases the computational cost of the convolution (which uses increasingly longer time periods) increases dramatically.

Trikha (1975) improved computation speed by approximating Zielke's weighting function using a sum of three exponential terms and formulating an approximate recursive relationship that eliminated the need for convolution (discussed in more detail in the following sections). The unsteady head loss for Trikha's formulation is

$$h_{fU}(t)_{app} = \frac{16\nu}{gD^2} \sum_{k=1}^{N} y_k(t) \tag{5}$$

where the variables y_k are defined as

$$y_k(t + \Delta t) = m_k \left[V(t + \Delta t) - V(t)\right] + e^{-n_k \Delta\tau} y_k(t) \tag{6}$$

and where N = number of exponential terms ($N = 3$ for the Trikha 1975 formulation), $\Delta\tau$ ($= 4\nu\Delta t/D^2$) is the dimensionless time step and n_k and m_k are coefficients of the exponential sum used to approximate the weighing function. The method requires the storing of N additional variables y_k at each space location in the MOC, but does not require costly convolutions. Although the approximation improved computational speed, this was at the expense of solution accuracy.

Following Trikha (1975), Kagawa *et al*. (1983) provided a more accurate solution by fitting a higher number of exponential terms (up to $N = 10$) to the weighting function for laminar flow.

The number of exponential terms used in the formulation depended on the value of $\Delta\tau$. The Kagawa *et al*. (1983) formulation uses Eq. 5, but the recursive expression for y_k is defined as

$$y_k\left(t+\Delta t\right)=m_k e^{-0.5n_k\Delta\tau}\left[V\left(t+\Delta t\right)-V\left(t\right)\right]+e^{-n_k\Delta\tau}y_k\left(t\right) \tag{7}$$

Suzuki *et al*. (1991) noticed that the original weighting function of Zielke (1968) already comprised an exponential part for $\tau > 0.02$. Therefore, the full convolution method was used for $\tau < 0.02$ and the Kagawa *et al*. (1983) approach was used for $\tau > 0.02$. However, for cases with $\Delta\tau << 0.02$ the majority of the analysis required full convolution for most applications, thus relinquishing efficiency gains. The Suzuki *et al*. (1991) formulation is as follows

$$h_{fU}\left(t\right)_{app}=\frac{16\nu}{gD^2}\sum_{j=1}^{M}\left[V\left(t-j\Delta t+\Delta t\right)-V\left(t-j\Delta t\right)\right]W\left(j\Delta t-\tfrac{1}{2}\Delta t\right)+\frac{16\nu}{gD^2}\sum_{k=1}^{5}y_k\left(t\right) \tag{8}$$

where the variables y_k are defined as

$$y_k\left(t+\Delta t\right)=e^{-n_k\Delta\tau\left(M+0.5\right)}\left[V\left(t-M\Delta t+\Delta t\right)-V\left(t-M\Delta t\right)\right]+e^{-n_k\Delta\tau}y_k\left(t\right) \tag{9}$$

and where M is equal to the maximum integer that does not exceed $(0.02/\Delta\tau + 0.5)$.

Schohl (1993) proposed a different recursive convolution algorithm that was derived by assuming the acceleration term in the convolution integral is constant between time steps, thus allowing full integration of the weighting function between time steps. The Schohl (1993) formulation uses Eq. 5, but the recursive expression for y_k is defined as

$$y_k\left(t+\Delta t\right)=\frac{m_k\left(1-e^{-n_k\Delta\tau}\right)}{n_k\Delta t}\left[V\left(t+\Delta t\right)-V\left(t\right)\right]+e^{-n_k\Delta\tau}y_k\left(t\right) \tag{10}$$

Whereas the previous recursive formulations were only applicable to laminar flows, Vítkovský *et al*. (2004) defined accurate approximations of the weighting function for laminar (Zielke 1968), smooth-pipe turbulent flows (Vardy and Brown 1995, 1996, 2003; Zarzycki

1997, 2000) and rough-pipe turbulent flows (Vardy and Brown 2004a). Like the Kagawa *et al*. (1983) approach, the number of exponential terms used in the weighting function approximation, N, depends on the value of $\Delta\tau$.

Sources of Error in Weighting Function-Based Models

One generally overlooked problem in the study of weighting function-based (WFB) unsteady friction models in pipe transients are the errors associated with the implementation of the WFB models and the effects of these errors on simulation. A list of different error types in WFB model implementation is as follows:

a) *Weighting Function Approximation Error*. The computation of unsteady friction using WFB models is most efficiently performed using the recursive convolution method. This method requires that the weighting function be approximated with a series of exponential functions. Error occurs when approximating the weighting function in such a way.
b) *Convolution Approximation Error*. WFB models are implemented as a weighting function convoluted with past accelerations. The integration in the convolution must be evaluated numerically in the finite difference grid and, therefore, is susceptible to error.
c) *Grid Separation Error*. Many formulations that apply WFB models in the MOC utilise a rectangular MOC grid. In these cases the WFB model ties together the two separate diamond grids that comprise the rectangular grid and, because each diamond grid is exposed to slightly different boundary conditions, causes a numerical oscillation in the simulation results.

Although the predominant method of transient analysis is the MOC, it should be noted that error types (a) and (b) would be common to other numerical schemes used for transient analysis, such as the Preissmann scheme; however, error type (c) is specific to the MOC scheme.

Finally, it should be noted that these error types are only related to the numerical application of WFB models in a finite difference grid. Additional error is made in the approximation of the true physical behaviour during the derivation of the weighting function approach. This error includes the applicability of the "frozen viscosity" assumption, the assumed viscosity profile, and the axi-symmetric flow assumption (Zielke 1968; Vardy and Brown 1995, 1996, 2003, 2004a; Zarzycki 1997, 2000). Additionally, error is generated when a simplified weighting function form is fitted to a wide range of Reynolds numbers and relative roughness (Vardy and Brown 1995, 1996, 2003, 2004a; Zarzycki 1997, 2000). Although most papers specify some error tolerance that was achieved during the fitting of the simplified weighting function, it is unclear what the actual effect of the simplification is on simulation results.

Weighting Functions used in Numerical Error Studies

The numerical error analyses presented in this paper can be applied to any weighting function. However, for the purposes of the present paper, the weighting function considered for the studies of numerical error is of the Vardy-Brown type. Vardy and Brown (1995) developed a weighting function in the form

$$W(\tau)_{true} = \frac{A^* e^{-B^*\tau}}{\sqrt{\tau}} \tag{11}$$

where A^* and B^* (= $1/C^*$, where C^* is the shear decay coefficient) are fitted coefficients to a more complex theoretical weighting function. For turbulent flows, A^* and B^* are dependent

on the Reynolds number (**Re**) of the instantaneous mean flow velocity and the relative roughness (ε/D). Vardy and Brown (2003) developed their coefficients for smooth pipe turbulent flow by linking the linearly varied frozen turbulent viscosity in the shear-layer with a uniform, but finite, viscosity in the core. The coefficients A^* and B^* were subsequently calculated as

$$A^* = \frac{1}{2\sqrt{\pi}}, \quad B^* = \frac{\mathbf{Re}^{\kappa}}{12.86} \quad \text{with} \quad \kappa = \log_{10}\left(15.29\mathbf{Re}^{-0.0567}\right) \tag{12}$$

The coefficients are valid for the range $2{,}000 < \mathbf{Re} < 10^8$. Additionally, Vardy and Brown (2004a) developed coefficients for fully-rough turbulent pipe flow as

$$A^* = 0.0103\sqrt{\mathbf{Re}}\left(\frac{\varepsilon}{D}\right)^{0.39} \quad \text{and} \quad B^* = 0.352\mathbf{Re}\left(\frac{\varepsilon}{D}\right)^{0.41} \tag{13}$$

The coefficients are valid for the range $10^{-6} < \varepsilon/D < 10^{-2}$.

Weighting Function Approximation Error

Due to the almost prohibitively slow computation of h_{fU} using the full convolution method (Zielke 1968), it is most advantageous to use the recursive convolution methods (Trikha 1975, Kagawa *et al*. 1983, Suzuki *et al*. 1991, Schohl 1993). The recursive convolution method relies on the approximation of the weighting function by a sum of exponential terms. The weighting function approximation is

$$W(\tau)_{app} = \sum_{k=1}^{N} m_k e^{-n_k \tau} \tag{14}$$

The coefficients of the exponential sum must be fitted such that the approximate weighting function resembles the true weighting function. Vítkovský *et al*. (2004) presented such approximations for laminar, smooth-pipe turbulent and rough-pipe turbulent weighting

functions. These approximations should be regarded as all-purpose or general in nature and have a high accuracy when an appropriate number of exponential terms are selected.

Allowing a small decrease in solution accuracy can save computational time. Consider the example pipeline in Figure 1 with the parameters for "Case #1" from Table 1. A transient event is generated by the instantaneous full closure of the valve from a fully open position. Two approximations of the weighting function are tested using three ($N = 3$) and ten ($N = 10$) exponential terms fitted in accordance with the procedure outlined in Vítkovský *et al*. (2004). The weighting function for each approximation is shown in Figure 2(a). The head response at the valve is shown in Figure 2(b) and demonstrates that even though a greatly reduced number of exponential terms are used in the $N = 3$ case, the simulation results are reasonable with respect to the true results.

The effect of the weighting function approximation error can be separated from the behaviour of the pipeline system by considering the unsteady head loss component of h_{fU} in the frequency domain. This error, E_A, is the ratio of the Fourier transforms of the approximate h_{fU} to the true h_{fU} and is

$$E_A(\omega') = \frac{\hat{W}(\omega')_{app}}{\hat{W}(\omega')_{true}} \tag{15}$$

where ω' = dimensionless angular frequency ($= \omega D^2/4\nu$) and "^" represents a Fourier transformed variable. The Fourier transforms of the true weighting function and the approximate weighting function are

$$\hat{W}(\omega')_{true} = A^* \sqrt{\frac{\pi}{B^* + i\omega'}} \quad \text{and} \quad \hat{W}(\omega')_{app} = \sum_{k=1}^{N} \frac{m_k}{n_k + i\omega'} \tag{16}$$

The magnitude of E_A represents the amount of damping caused by the approximation, while the argument of E_A represents the difference in phase. Figure 3 shows E_A for the $N = 3$ and

$N = 10$ approximations of the weighting function and shows that W is well approximated by the $N = 3$ case for small ω' (i.e., low frequencies), but not for large ω' (i.e., high frequencies). However, transient events, such as a valve closure, comprise predominantly low frequency components with less significant magnitude high frequency components. Therefore, for a valve closure event, errors in the weighting function in the high frequency range have less effect than errors in the weighting function in the low frequency range. This behaviour is explained in more detail later in the paper.

While the approximation of the weighting function shown in Vítkovský *et al*. (2004) applied over a large τ range and for up to 10 exponential terms, it is possible to tune the approximation of the weighting function (in terms of the τ range and number of exponential terms) to a particular problem for both accuracy and efficiency. Because there are two competing objectives, namely the approximation accuracy and computational efficiency, a single solution does not exist. Rather, there is an optimal front of solutions. The number of exponential terms (N) used in the weighting function approximation is a good surrogate for the computational efficiency. The accuracy of the weighting function approximation can be defined in a number of different ways, two of which are considered in this paper. The first measure of accuracy is the sum of the squares of the relative errors in the weighting function (E_W),

$$E_W = \sum_{j=1}^{M} \left[\frac{W(\tau_j)_{true} - W(\tau_j)_{app}}{W(\tau_j)_{app}} \right]^2 \tag{17}$$

where W_{true} = true weighting function, and W_{app} = approximate weighting function. The measure E_W is the objective function used to fit the parameters of the approximate weighting function (Eq. 14). The second measure of accuracy is the sum of the squares of the standardised head response error (E_H),

$$E_H = \sum_{j=1}^{M} \left[\frac{H(t_j)_{true} - H(t_j)_{app}}{H_{ref}} \right]^2 \tag{18}$$

where H_{true} = true head response using W_{true}, H_{app} = approximate head response using W_{app}, and H_{ref} = reference head that is non-zero and representative of the pressure in the system. Essentially, the difference between E_W and E_H is that fitting with E_W does not assume anything about the transient event, while on the other hand; fitting with E_H depends on the characteristics of the transient event. Hence, an optimal weighting function fitted with E_H for one transient event will be sub-optimal for different transient event. Fitting the weighting function with E_W generally gives more robust results in terms of the simulation of a range of transient events. The parameters for the approximation of the weighting function are the number of exponential terms (N) and the τ range $[\tau_{min}, \tau_{max}]$. For a particular transient problem, the lower bound of the τ range is defined by the time step used in the simulation (i.e., $\tau_{min} = 4\nu\Delta t/D^2$). The upper bound of the τ range τ_{max} may be based on the total simulation time (i.e., $\tau_{max} = 4\nu T/D^2$, where T is the total simulation time), but this results in an overly conservative estimate (as shown later). Subsequently, the upper bound τ_{max} and N remain to be determined.

For the transient problem under consideration, an investigation into the approximation accuracy and computational efficiency has been performed. The reference head H_{ref} is chosen as the initial pressure at the valve preceding the transient event. The lower bound of the τ range is set as $\tau_{min} = 10^{-6}$. The exponential coefficients are fitted for all combinations of $N = \{1, 2, 3, 4, 5, 6, 7, 8, 9, 10\}$ and $\tau_{max} = \{10^{-5}, 10^{-4}, 10^{-3}, 10^{-2}, 10^{-1}\}$. Figure 4(a) shows the values of E_W for different values of N and τ_{max}. Generally speaking, the greater the number of exponential terms, and the smaller the τ range, the better the weighting function approximation (i.e., the lower E_W).

A more interesting set of curves is found in Figure 4(b), in which the accuracy of the head response is considered (using E_H) based on the fits using E_W. Ultimately, the accuracy measure based on the head response (E_H) is the more important for transient simulation. Figure 4(b) shows that given a particular number of exponential terms there exists a maximum accuracy (minimum value of E_H) when $\tau_{max} \approx 10^{-3}$. This value corresponds to the point at which $W(\tau_{min})/W(\tau_{max}) \approx 10^3$, and suggests that contributions to unsteady friction for large τ_{max} are small given that $W(\tau_{min}) >> W(\tau_{max})$. Therefore, since τ_{min} is defined by the computational time step, τ_{max} can be defined by the point at which $W(\tau_{min})/W(\tau_{max}) \approx 10^3$. The main factor that influences the ratio $W(\tau_{min})/W(\tau_{max})$, and hence the determination of τ_{max}, is the parameter B^* in the weighting function (Eq. 11). Figure 5(a) shows the variation of B^* with the Reynolds number (**Re**) of the flow and the relative roughness (ε/D) of the pipe. As **Re** and ε/D increase, the value of B^* increases, with the resulting weighting function becoming steeper, and thus reducing the size of the τ range required. Figure 5(b) shows the relationship between τ_{min} and τ_{max} (and hence the τ range) for a given value of B^* such that $W(\tau_{min})/W(\tau_{max}) = 10^3$. Together, Figure 5(a) and Figure 5(b) define a reasonable τ range for transient simulation. An adequate number of exponential terms can be determined by increasing from $N = 1$ until a prescribed level of accuracy has been achieved (see Figure 4(b)). A procedure to tune the parameters of the weighting function approximation for both efficiency and accuracy for a particular transient event is:

1. Define τ_{min} as equal to the dimensionless time step $\Delta\tau$.
2. Calculate B^* from **Re** and ε/D for the particular initial flow conditions and pipe roughness using the appropriate Eq. 12 or 13.
3. Determine a reasonable τ_{max} using Figure 5(b).

4. Using Eq. 18 to define an error for the particular transient event, increase the number of exponential terms from $N = 1$ until a prescribed level of accuracy, as defined by the engineer or required by the application, is attained.

While the original version of this paper was under review, Vardy and Brown (2004b) presented a paper that also considered the trade-off between the number of exponential terms and the accuracy of the weighting function approximation. Their approach for fitting the exponential terms was quite efficient and did not require the use of a minimization algorithm. However, their approach did require an assumption as to the location of the points of coincidence between the true and approximate weighting functions (knots). The approach used in the present paper for the fitting of the exponential terms was based on a minimization algorithm and, although more time consuming, does not make such an assumption. It should be noted that the weighting function approximation in Vítkovský *et al*. (2004) uses a scaling-approach and does not require re-fitting (by minimisation) for different Reynolds numbers flows and pipe relative roughnesses, whereas the Vardy and Brown (2004b) approach does require re-fitting.

Convolution Approximation Error

A source of numerical error in the implementation of WFB models that is typically overlooked is the approximation of the convolution of the weighting function with the fluid acceleration. Evaluation of error in the convolution is fundamental, since even the most brilliantly derived weighting function can be rendered useless by poor convolution implementation. This error is best assessed in the frequency domain where the convolution integral can be evaluated exactly and used as a benchmark. A measure of the convolution

error, E_C, can be defined as the ratio of the "approximate" and "true" Fourier transforms of the unsteady head loss component h_{fU} (see Eq. 3) as

$$E_C(\omega) = \frac{\hat{h}_{fU}(\omega)_{app}}{\hat{h}_{fU}(\omega)_{true}} \tag{19}$$

The quantity E_C represents the convolution approximation error and is a function of the frequency of disturbance, grid spacing in time and the weighting function. The absolute value and argument of E_C define the magnitude and phase errors associated with the convolution approximation error. Determination of E_C requires that $h_{fU}(t)_{app}$ for the recursive convolution algorithms be written in a full convolution form. This is achieved by successively substituting y_k into h_{fU} resulting in an infinite sum that, in the limit, does not depend on y_k.

The convolution approximation error for the Zielke (1968) convolution algorithm is

$$E_C(\omega) = \mathrm{sinc}\left(\frac{\omega\Delta t}{\pi}\right)\frac{2\Delta t\sum_{j=1,3,5,\ldots}^{\infty} e^{-i\omega j\Delta t}W(j\Delta t)}{\hat{W}(\omega)} \tag{20}$$

where $\mathrm{sinc}(x)=\sin(\pi x)/(\pi x)$ and is commonly termed the "sampling function." The convolution approximation error for the Trikha (1975) recursive algorithm is

$$E_C(\omega) = \mathrm{sinc}\left(\frac{\omega\Delta t}{2\pi}\right)\frac{\Delta t\sum_{j=1,2,3,\ldots}^{\infty} e^{-i\omega(j\Delta t-0.5\Delta t)}W(j\Delta t-\Delta t)}{\hat{W}(\omega)} \tag{21}$$

The convolution approximation error for the Kagawa *et al*. (1983) and Suzuki *et al*. (1991) recursive algorithms is

$$E_C(\omega) = \mathrm{sinc}\left(\frac{\omega\Delta t}{2\pi}\right)\frac{\Delta t\sum_{j=1,2,3,\ldots}^{\infty} e^{-i\omega(j\Delta t-0.5\Delta t)}W(j\Delta t-0.5\Delta t)}{\hat{W}(\omega)} \tag{22}$$

The convolution approximation error for the Schohl (1993) recursive algorithm is

$$E_C(\omega) = \mathrm{sinc}\left(\frac{\omega\Delta t}{2\pi}\right)\frac{\sum_{j=1,2,3,\ldots}^{\infty}\left[e^{-i\omega(j\Delta t-0.5\Delta t)}\int_{j\Delta t-\Delta t}^{j\Delta t}W(t^*)dt^*\right]}{\hat{W}(\omega)} \tag{23}$$

Note that all formulae for h_{fU} and E_C are given in terms of a generic weighting function W even though all recursive algorithms are only designed for weighting functions comprising a sum of exponential terms.

As an example, the smooth-pipe turbulent weighting function (Eq. 12) with a Reynolds number of 10,000 is used for calculation of E_C. Figure 6 shows both the magnitude and phase errors of the convolution approximation error for the different convolution algorithms. The analysis is given in terms of the dimensionless frequency ratio ω/ω_{grid} where ω_{grid} is the angular frequency of the grid ($\omega_{grid} = 2\pi/\Delta t$).

The Trikha (1975) algorithm performs poorly and approaches the error of the other algorithms only for the smallest dimensionless time step ($\Delta\tau = 10^{-6}$). The Zielke (1968) algorithm performs slightly worse than the Kagawa *et al*. (1983) and Suzuki *et al*. (1991) algorithms. This is because the Zielke (1968) algorithm is applied at double the time step. The Schohl (1993) algorithm performs the best out of all the algorithms and exhibits nearly zero magnitude error for most frequencies other than those at the high end of the range ($\omega/\omega_{grid} > 2\times10^{-2}$).

The analysis outlines an important point when using the Zielke (1968), Kagawa *et al*. (1983) and Suzuki *et al*. (1991) algorithms, in that having a coarsely discretised grid, such as in large pipeline or network analysis, will result in the unsteady head loss being artificially reduced due to approximation in the convolution integral.

Grid Separation Error

The Trikha (1975), Kagawa *et al*. (1983), Suzuki *et al*. (1991), and Schohl (1993) formulations are all implemented on rectangular MOC grids. The rectangular grid comprises two interlaced diamond grids, each of which experience slightly different boundary conditions. The different boundary conditions imposed on each diamond grid results in a slightly different transient response in each grid. An unsteady friction model that utilises points from both diamond grids ties together the two separate diamond grids. The mismatch in the transient response between each diamond grid (within the rectangular grid) results in a grid separation problem that induces a numerical error near sharp features in the transient with a frequency of the grid spacing. A time-domain representation of grid separation error was presented in Vítkovský *et al*. (2004). Ideally, errors resulting from grid separation should be avoided.

Consideration of the unsteady head loss due a sharp step-change in velocity leads to an analytically derived error associated with grid separation. Ideally, the velocity series used in numerical convolution algorithms would be written as

$$\widetilde{V}(t) = \{V(t), V(t-\Delta t), V(t-2\Delta t), V(t-3\Delta t), V(t-4\Delta t), \ldots\} \tag{24}$$

However after a sharp step-event, the velocity series resembles two identical series sampled at $2\Delta t$ (corresponding to each interlaced diamond grid that comprises the rectangular grid) that are out of phase by Δt (the step-change is registered by one rectangular grid one time step later than the other). Such a velocity series can be written as

$$\widetilde{V}_1(t) = \{V(t), V(t-2\Delta t), V(t-2\Delta t), V(t-4\Delta t), V(t-4\Delta t), \ldots\} \tag{25}$$

One time step later the velocity series becomes

$$\widetilde{V}_2(t) = \{V(t), V(t), V(t-2\Delta t), V(t-2\Delta t), V(t-4\Delta t), \ldots\} \tag{26}$$

Substitution of the velocity series $\widetilde{V}_1$ and $\widetilde{V}_2$ into the unsteady head loss equation (Eq. 3) results in two alternate magnitudes of unsteady frictional loss $h_{fU}\left(\widetilde{V}_1,t\right)$ and $h_{fU}\left(\widetilde{V}_2,t\right)$, respectively. The mismatch in these alternate head loss magnitudes is observed as an oscillation with a period of $2\Delta t$ (equal to the highest frequency possible in a rectangular grid). Similar to E_C, the determination of E_G requires that $h_{fU}(t)_{app}$ for the recursive convolution algorithms be written first in a full convolution form. The grid separation error, E_G, can be defined as the ratio of the Fourier transforms of the unsteady head loss for velocity series $\widetilde{V}_1$ and $\widetilde{V}_2$, and is written as

$$E_G(\omega)=\frac{\hat{h}_{fU}\left(\widetilde{V}_2,\omega\right)_{app}}{\hat{h}_{fU}\left(\widetilde{V}_1,\omega\right)_{app}} \tag{27}$$

The grid separation error for the Trikha (1975) algorithm is

$$E_G(\omega)=\frac{e^{i\omega\Delta t}\sum_{j=2,4,6,\ldots}^{\infty}e^{-i\omega j\Delta t}W\left(j\Delta t-\Delta t\right)}{\sum_{j=1,3,5,\ldots}^{\infty}e^{-i\omega j\Delta t}W\left(j\Delta t-\Delta t\right)} \tag{28}$$

The grid separation error for Kagawa *et al*. (1983) and Suzuki *et al*. (1991) algorithms is

$$E_G(\omega)=\frac{e^{i\omega\Delta t}\sum_{j=2,4,6,\ldots}^{\infty}e^{-i\omega j\Delta t}W\left(j\Delta t-0.5\Delta t\right)}{\sum_{j=1,3,5,\ldots}^{\infty}e^{-i\omega j\Delta t}W\left(j\Delta t-0.5\Delta t\right)} \tag{29}$$

The grid separation error for the Schohl (1993) algorithm is

$$E_G(\omega)=\frac{e^{i\omega\Delta t}\sum_{j=2,4,6,\ldots}^{\infty}\left[e^{-i\omega j\Delta t}\int_{j\Delta t-\Delta t}^{j\Delta t}W\left(t^*\right)dt^*\right]}{\sum_{j=1,3,5,\ldots}^{\infty}\left[e^{-i\omega j\Delta t}\int_{j\Delta t-\Delta t}^{j\Delta t}W\left(t^*\right)dt^*\right]} \tag{30}$$

It should be noted that the full grid separation error is realised for a short period after a sharp change in the boundary conditions. The error resembles a high frequency oscillation with a period of $2\Delta t$, however, the effect of unsteady friction is to attenuate those high frequency components of a transient and hence the grid separation error persists only for a short amount of time (generally three or four transient cycles).

Figure 7 shows plots of E_G versus the dimensionless frequency ratio ω/ω_{grid}. Because each velocity series relates to each diamond grid, the maximum possible frequency is limited to $\omega/\omega_{grid} = ¼$ (even though the grid separation error is observed with a frequency of $\omega/\omega_{grid} = ½$). The results show that the Trikha (1975) algorithm produces the greatest grid separation error and approaches the behaviour of the Kagawa *et al*. (1983) and Suzuki *et al*. (1991) algorithms for the smallest dimensionless time step ($\Delta\tau = 10^{-6}$). The Schohl (1993) algorithm shows more grid separation error (both in magnitude and phase) than the Kagawa *et al*. (1983) and Suzuki *et al*. (1991) algorithms.

An interesting observation is that more finely discretising the MOC grid (decreasing $\Delta\tau$) does not affect the magnitude of the error as the error magnitude approaches a limit for small $\Delta\tau$. More finely discretising the MOC grid only causes the frequency of the grid separation disturbance to increase.

Improvement to Recursive Algorithms

A simple approach to reduce errors associated with grid separation is to apply the Kagawa *et al*. (1983) and Schohl (1993) formulations (Eqs. 7 and 10, respectively) on a diamond grid rather than on a rectangular grid (i.e., a time step of $2\Delta t$). Doing this eliminates grid

separation error at the expense of a small increase in convolution approximation error. The Kagawa *et al*. (1983) recursive formulation applied to a diamond grid is

$$y_k(t+2\Delta t) = m_k e^{-n_k \Delta\tau}\left[V(t+2\Delta t) - V(t)\right] + e^{-2n_k \Delta\tau} y_k(t) \tag{31}$$

The Schohl (1993) recursive formulation applied to a diamond grid is

$$y_k(t+2\Delta t) = \frac{m_k\left(1-e^{-2n_k \Delta\tau}\right)}{2n_k \Delta\tau}\left[V(t+2\Delta t) - V(t)\right] + e^{-2n_k \Delta\tau} y_k(t) \tag{32}$$

Both formulations still use Eq. 5 for the summation of the y_k terms.

The convolution approximation error for Eqs. 31 and 32 give similar performance to their rectangular grid counterparts (Eqs. 22 and 23 respectively). The convolution approximation error for the Kagawa *et al*. (1983) algorithm applied to a diamond grid is identical to that of Zielke (1968), and hence given by Eq. 20. The convolution approximation error for the Schohl (1993) algorithm applied to a diamond grid is

$$E_C(\omega) = \operatorname{sinc}\left(\frac{\omega\Delta t}{\pi}\right)\frac{\sum_{j=1,3,5,\ldots}^{\infty}\left[e^{-i\omega j\Delta t}\int_{j\Delta t-\Delta t}^{j\Delta t+\Delta t} W(t^*)dt^*\right]}{\hat{W}(\omega)} \tag{33}$$

Significance of Weighting Function-Based Model Error in Transient Systems

The previous section in this paper dealt with the different types of errors that afflict the implementation of WFB unsteady friction models. However, in terms of the transient analysis of a complete pipeline system, the effect of any numerical errors in unsteady friction, and indeed unsteady friction itself, might be less important than first imagined. The following sections consider the magnitude of quasi-steady friction, input bandwidth, system bandwidth

and system component dominance with respect to unsteady friction in a complete pipeline system.

Quasi-Steady Friction vs Unsteady Friction Dominance

The relative magnitudes of quasi-steady and unsteady friction is a topic of importance since it provides a basis upon which to decide whether or not it is necessary to model unsteady friction accurately or even at all. During a transient event many different frequency components are present. Unsteady friction affects the higher frequency components through extra attenuation and dispersion. Those transient events whose energy spectrum is distributed in the higher frequency range are susceptible to greater attenuation and dispersion caused by unsteady friction. It therefore becomes important to define which frequency components are affected by unsteady friction.

The effect of the unsteady friction component in the total unsteady head loss (comprising quasi-steady and unsteady frictional components) is a function of frequency and can be demonstrated by determining the ratio of the Fourier transforms of the total unsteady head loss and the quasi-steady head loss. This ratio, R_F, is

$$R_F(\omega') = \frac{\hat{h}_{fS}(\omega') + \hat{h}_{fU}(\omega')}{\hat{h}_{fS}(\omega')} = 1 + \frac{i\omega' 32}{f_0 \mathbf{Re}_0} \hat{W}_0(\omega') \tag{34}$$

Note that the quasi-steady friction term has been linearised as $h_{fS} = (f_0|V_0|/2gD)V$. The Fourier transform of the weighting function has been previously given in Eq. 16. The absolute value of R_F represents the ratio of the total unsteady head loss to the quasi-steady friction component head loss. The argument of R_F represents the phase difference between the average velocity and the unsteady friction component (since the quasi-steady friction

component is exactly in-phase with the average velocity). Note that as the frequency ω' approaches zero R_F approaches a value of one. Thus the total unsteady dissipation approaches the steady-state dissipation and becomes increasingly in-phase with the average velocity. Figure 8 shows the variation of R_F with dimensionless frequency for a range of Reynolds numbers (the smooth-pipe turbulent weighting function formula is used, Eq. 12—note that a similar, but different, set of curves can be generated for rough pipes using Eqs. 34 and 13). Components with higher dimensionless frequencies and lower Reynolds numbers experience significant extra attenuation caused by unsteady friction. The value of R_F can be used to define which type of friction is dominant.

In terms of the example pipeline shown in Figure 1, after the valve closure the fluid freely vibrates until a zero flow condition is reached. The dimensionless fundamental frequency, ω'_{th}, of the transient response for an open-closed pipeline system is

$$\omega'_{th} = \frac{\pi a D^2}{8 L \nu} \tag{35}$$

The dimensionless fundamental frequency represents the lower end of the frequency range in the transient response and therefore gives a conservative estimate of the unsteady friction damping. For Case #1 ($\mathbf{Re}_0 = 6{,}564$) the dimensionless fundamental frequency is 6,765 rad, which corresponds to a total unsteady/quasi-steady friction ratio of approximately six (see Figure 8), meaning that the system is indeed unsteady friction dominant. It should be noted that larger diameter pipelines tend to have larger dimensionless fundamental frequencies, which suggests that larger pipelines will have greater unsteady friction damping. However, this is true only if the flow in the larger pipeline has a low Reynolds number and the length of the pipeline is short. As the Reynolds number of the flow increases the total unsteady/quasi-steady friction ratio decreases. A similar behaviour is observed for pipelines with increasing relative roughness. An interesting observation from Eq. 35 is that $\omega'_{th} \propto \nu^{-1}$, thus for higher

viscosity liquids the relative affect of unsteady friction compared to quasi-steady friction lessens.

Limited Input Bandwidth

For a given pipeline system, an input to the system and an output from the system can be identified. Treating the pipeline system in such a way can aid in the interpretation of unsteady friction with regard to system input. For small perturbations a transient system can be approximated as a linear system. For a linear system the input and output are related by the impulse response function as

$$H(t) = (\Theta * V)(t) \tag{36}$$

where (in this case) the input is the velocity V, the output is the head H, and Θ is the impulse response function. A property of a linear system is that if the input is decomposed into a number of different frequency sinusoids, then the system acts on each sinusoidal component independently and the output can be recomposed from these modified components. The Fourier transform of the input performs such decomposition in the frequency domain. Consequently, if a system input is deficient in high frequency components, then the output will be generally deficient in high frequency components too. This behaviour has implications with respect to the potential effect of unsteady friction. As shown in the previous section, the effect of unsteady friction becomes greater as the frequency of the disturbance increases (Figure 8). If the system input has limited input bandwidth then the effects of unsteady friction lose importance in the system response.

Input bandwidth relates to the spectrum of the input in the frequency domain and is the frequency range that contains the majority of the input power. The effect of limited input

bandwidth is best illustrated by example. An example pipeline system, as shown in Figure 1, has the velocity at the valve as an input and the head at the valve as an output. This arrangement was chosen because the system comprises only linear components except for, ironically, quasi-steady friction that is non-linear. The parameters for this system are shown in Table 1 as "Case #2" and the system arrangement resembles Figure 1. The input to the system is an initially steady velocity that is reduced to zero with a cosine profile over the time periods 0.1 and 4.0 seconds. The time-domain representation and frequency-domain representations of the input are shown in Figure 9. As observed, the input with a 0.1 s time period has greater amplitude high frequency components than the signal with a 4.0 s period, and are named the high bandwidth and low bandwidth respectively. Figure 10 shows the output produced from the high and low bandwidth inputs. The output from the high bandwidth input shows a relatively higher unsteady friction effect than the output from the low bandwidth input. In fact, for the low bandwidth input and this particular system configuration, good simulation results could be computed with quasi-steady friction alone. However, this result is particular to this system configuration and may not be applicable to others for a similar low bandwidth input. Ultimately, modelling with unsteady friction regardless of the input bandwidth is always preferable to modelling with quasi-steady friction only.

Limited System Bandwidth and System Component Dominance

There are two ways the system can affect unsteady friction. The first is by effectively applying a bandwidth to the system behaviour. The second is by having system components that produce behaviour that is more dominant than unsteady friction. In these cases it could be argued that if there exists a more dominant system component than unsteady friction or the

system effectively limits the bandwidth (by damping out the high frequency components) of the transient then unsteady friction need only be approximately modelled. Again, the linear system approach can be used to demonstrate these effects. The Fourier transform of Eq. 36 is

$$\hat{H}(\omega) = \hat{\Theta}(\omega)\hat{V}(\omega) \tag{37}$$

where $\hat{\Theta}$ is the transfer function of the system. In a linear system the transfer function acts on each frequency component of the input independently to form the output. Therefore, the transfer function for the system can show the behaviour of the system irrespective of the input to the system.

System component dominance is demonstrated by numerical example using the pipeline system from the previous section (Case #2). The high bandwidth input is used from the previous section, but the pipeline material has been changed to that which exhibits viscoelastic behaviour. The creep compliance function for the pipe material used in the numerical example is for medium density PVC at 25°C from Galley *et al*. (1979). Figure 11 shows the transfer function for the pipeline system for the cases of (a) unsteady friction only, (b) viscoelastic material only and (c) unsteady friction and viscoelastic material together. The results that contain the viscoelastic material show significant damping above a frequency of 20 rad/s and effectively limit the output bandwidth to approximately 20 rad/s. The transfer function for both unsteady friction and the viscoelastic material together is similar to that of the viscoelastic material alone. These observations from the transfer function are confirmed in the head response at the valve, as shown in Figure 12. In this particular case, the viscoelastic material damping behaviour is much more dominant than that of unsteady friction. Additionally, the viscoelastic material limits the system bandwidth further reducing the affect of unsteady friction by eliminating the higher frequency components of the

transient. It could be argued that in this case the unsteady friction need only be modelled approximately, although this may not be the case generally.

Conclusions

A topic of research that has been generally neglected in the literature is the analysis of error in the numerical implementation of weighting function-based unsteady friction models. This paper has presented an analysis of error with respect to the numerical implementation of weighting function-based models and the significance of that error in the context of modelling transients in a pipeline system. All error analyses have been performed in the frequency domain where analytical solutions can be determined.

The performance of a number of different numerical unsteady friction implementation schemes has been considered, including those of Zielke (1968), Trikha (1975), Kagawa *et al*. (1983), Suzuki *et al*. (1991) and Schohl (1993). Three new measures of numerical error have been defined: (i) weighting function approximation error, (ii) convolution approximation error and (iii) grid separation error. The first two error measures are applicable to any finite difference scheme, whereas the third error measure is only applicable to the method of characteristics.

The use of efficient recursive algorithms requires the approximation of the weighting function by a number of exponential terms. The weighting function approximation error has been found to be a trade-off between number of computational terms and accuracy of the weighting function approximation. A procedure has been defined to fit the exponential sum to the weighting function based on an optimisation approach. Also, the fitting of the weighting

function could be performed using either in the time domain or frequency domain criteria depending on the desired result.

The convolution approximation error analysis for each implementation scheme showed that the Schohl (1993) algorithm showed the least amount of error, and only produced small error for large dimensionless frequency ratios. The Trikha (1975) algorithm produced the worst errors, while the Zielke (1968), Kagawa *et al*. (1983) and Suzuki *et al*. (1991) algorithms showed problems when using larger dimensionless time steps. It should be acknowledged that the unsteady friction modelling field is indebted to Trikha for initiating the study of efficiency in simulation. That said, Trikha's algorithm is not suitable for systems with realistic time steps and better algorithms have existed for an amount of time, but many researchers still persist with Trikha's algorithm without realising the error they are introducing into their work.

The grid separation error analysis for each implementation (those applied on a rectangular grid system) showed that the Kagawa *et al*. (1983) and Suzuki *et al*. (1991) algorithms showed the least error, followed by the Schohl (1993) and Trikha (1975) algorithms. Simply applying each algorithm on a diamond grid system solved grid separation problems.

Four different effects have been defined to explain the significance of errors in unsteady friction computation in the context of pipeline systems. The effects were (i) unsteady/quasi-steady friction dominance, (ii) limited input bandwidth, (iii) limited system bandwidth, and (iv) system component dominance.

The ratio of unsteady to quasi-steady friction losses showed that unsteady friction could be far more dominant than quasi-steady friction for even low dimensionless frequencies given a low Reynolds number. The fundamental dimensionless frequency of closed-open pipelines could be used to test whether or not a pipeline is dominated by quasi-steady or unsteady friction.

The effect of input bandwidth could be assessed based on the spectrum of the transient input. If the input bandwidth to the pipeline system is low then errors in the unsteady friction for high frequencies affected the simulation results less. In some cases, if the input bandwidth is very low then the impact of unsteady friction, as a whole, is almost negligible.

It was observed that the characteristics of the pipeline system could affect the significance of unsteady friction and its approximation. The transfer function of the pipeline system was utilised for this purpose. Systems that contained components with large associated damping behaviour could dominate unsteady friction. Additionally, system components, such as a viscoelastic pipe material, could effectively apply a bandwidth to the transient reducing the effect of unsteady friction at higher frequencies (where unsteady friction is more dominant).

Finally, the study of the significance of unsteady friction errors in pipeline systems showed that the need to model unsteady friction should be assessed on a case-by-case basis depending on the input and system characteristics before deciding to neglect it from analysis.

Acknowledgements

The writers would like to acknowledge financial support from the Australian Research Council and a scholarship provided by the Australian Government for the second author. Both sources of assistance are gratefully appreciated.

Notation

A^*, B^* = Vardy-Brown weighting function coefficients;

a = wave speed;

D = pipe diameter;

E_A = weighting function approximation error;

E_C = convolution approximation error;

E_G = grid separation error;

E_H = standardised error in head response;

E_W = relative error in weighting function;

f = Darcy-Weisbach friction factor;

g = gravitational acceleration;

H = head;

h_{fS} = quasi-steady component of total unsteady head loss per unit length;

h_{fU} = unsteady component of total unsteady head loss per unit length;

i = imaginary unit $\left(=\sqrt{-1}\right)$;

L = pipe length;

M = number of points in E_W and E_H calculation; = $t/\Delta t - 1$; = int$(0.02/\Delta\tau + 0.5)$;

N = number of exponential terms;

n_k, m_k = exponential sum coefficients;

Re = Reynolds number;

R_F = frequency domain total unsteady/quasi-steady head loss ratio;

T = total simulation time;

t = time;

V = average velocity;

W = weighting function;

y_k = extra coefficient for proposed method;

ε = pipe wall roughness;

Δt = time step;

$\Delta\tau$ = dimensionless time step ($= 4\nu\Delta t/D^2$);

ν = kinematic viscosity;

ρ = mass density of liquid;

τ = dimensionless time ($= 4\nu t/D^2$);

τ_{min} = lower bound for dimensionless time range;

τ_{max} = upper bound for dimensionless time range;

θ = angle of inclination of the pipe to the horizontal;

Θ = system impulse response function;

ω = angular frequency;

ω_{grid} = grid angular frequency ($=2\pi/\Delta t$)

ω' = dimensionless angular frequency ($= \omega D^2/(4\nu)$);

ω'_{th} = dimensionless angular fundamental frequency for an open-closed pipeline system;

Subscripts:

0 = initial or steady-state quantity

app = approximate quantity

ref = reference quantity;

true = true or exact quantity

Superscripts:

^ = Fourier transformed quantity

~ = Representing a series

References

Ghidaoui, M.S., and Mansour, S. (2002). "Efficient Treatment of Vardy-Brown Unsteady Shear in Pipe Transients." *Journal of Hydraulic Engineering*, ASCE, 128(1), January, 102-112.

Gally, M., Güney, M., and Rieuford, E. (1979). "An Investigation of Pressure Transients in Viscoelastic Pipes." *Journal of Fluids Engineering*, Transactions of the ASME, 101, December, 495-499.

Kagawa, T., Lee, I., Kitagawa, A., and Takenaka, T. (1983). "High Speed and Accurate Computing Method of Frequency-Dependent Friction in Laminar Pipe Flow for Characteristics Method." *Transactions of the Japanese Society of Mechanical Engineers*, 49(447), 2638-2644. (in Japanese)

Pezzinga, G. (1999). "Quasi-2D Model for Unsteady Flow in Pipe Networks." *Journal of Hydraulic Engineering*, ASCE, 125(7), 676-685.

Schohl, G.A. (1993). "Improved Approximate Method for Simulation Frequency-Dependent Friction in Transient Laminar Flow." *Journal of Fluids Engineering*, Transactions of the ASME, 115, September, 420-424.

Suzuki, K., Taketomi, T., and Sato, S. (1991). "Improving Zielke's Method of Simulating Frequency-Dependent Friction in Laminar Liquid Pipe Flow." *Journal of Fluids Engineering*, Transactions of the ASME, 113, 569-573.

Trikha, A.K. (1975). "An Efficient Method for Simulating Frequency-Dependent Friction in Transient Liquid Flow." *Journal of Fluids Engineering*, Transactions of the ASME, 97, 97-105.

Vardy, A.E., and Brown, J.M. (1995). "Transient, Turbulent, Smooth Pipe Friction." *Journal of Hydraulic Research*, IAHR, 33(4), 435-456.

Vardy, A.E., and Brown, J.M. (1996). "On Turbulent, Unsteady, Smooth Pipe Friction." *7th International Conference on Pressure Surges and Fluid Transients in Pipelines and Open Channels*, BHR Group, Harrogate, UK, April, 289-311.

Vardy, A.E., and Brown, J.M.B. (2003). "Transient Turbulent Friction in Smooth Pipe Flows." *Journal of Sound and Vibration*, 259, 1011-1036.

Vardy, A.E., and Brown, J.M.B. (2004a). "Transient Turbulent Friction in Fully-Rough Pipe Flows." *Journal of Sound and Vibration*, 270, 233-257.

Vardy, A.E., and Brown, J.M.B. (2004b). "Efficient Approximation of Unsteady Friction Weighting Functions." *Journal of Hydraulic Engineering*, ASCE, 130(11), November, 1097-1107.

Vardy, A.E., and Hwang, K.-L. (1991). "A Characteristics Model of Transient Friction in Pipes." *Journal of Hydraulic Research*, IAHR, 29(5), 669-684.

Vítkovský, J.P., Stephens, M.L., Bergant, A., Lambert, M.F., and Simpson, A.R. (2004). "Efficient and Accurate Calculation of Zielke and Vardy-Brown Unsteady Friction in Pipe Transients." *9th International Conference on Pressure Surges*, BHR Group, 24-26 March, Chester, UK, Volume 2, 405-419.

Wylie, E.B., and Streeter, V.L. (1993). *Fluid Transients in Systems*. Prentice-Hall Inc., Englewood Cliffs, New Jersey, USA.

Zarzycki, Z. (1997). "Hydraulic Resistance of Unsteady Turbulent Liquid Flow in Pipes." *Water Pipeline Systems*, BHR Group, 163-178.

Zarzycki, Z. (2000). "On Weighting Function for Wall Shear Stress During Unsteady Turbulent Pipe Flow." *8th International Conference on Pressure Surges*, BHR Group, The Hague, The Netherlands, 12-14 April.

Zielke, W. (1968). "Frequency-Dependent Friction in Transient Pipe Flow." *Journal of Basic Engineering*, Transactions of the ASME, 90(1), 109-115.

List of Tables and Figures

[Note that all figures are sized to exactly fit into one column as specified by the ASCE Author's Guide. Alternatively, figures with two components could be rearranged to be side-by-side and would fit exactly into one page width.]

Table 1. Parameters for example pipeline systems

Case #1 Parameters	Case #2 Parameters	Common Parameters
D = 22.1 mm	D = 50.0 mm	g = 9.81 m/s^2
L = 37.2 m	L = 200.0 m	ρ = 998.2 kg/m^3
a = 1319.0 m/s	a_0 = 366.7 m/s	$\nu = 1.01\times10^{-6}$ m^2/s
ε = 0.0015 mm	ε = 0.005 mm	V_0 = 0.3 m/s
$\mathbf{Re}_0$ = 6,564	$\mathbf{Re}_0$ = 14,851	H_0 at Tank 2 = 30 m

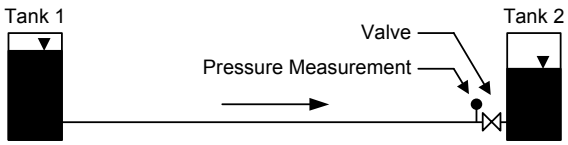

Figure 1. Example pipeline definition

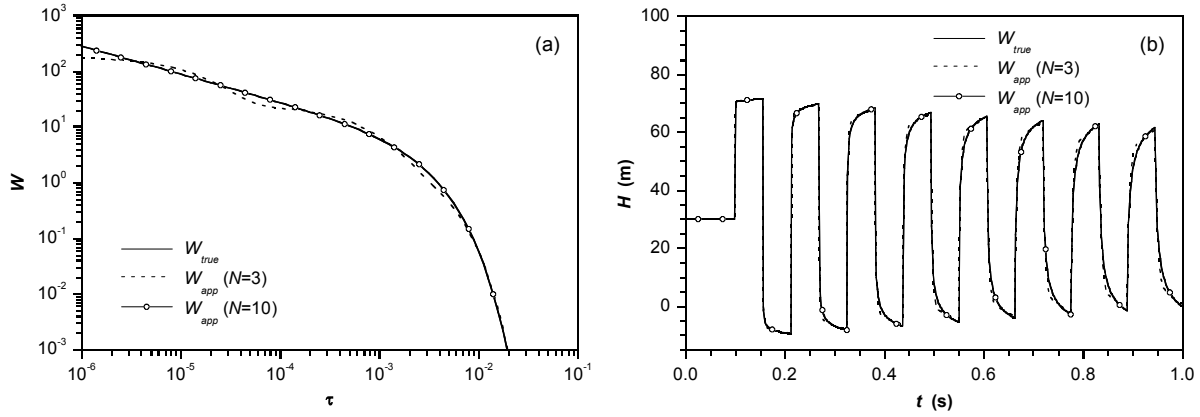

Figure 2. Example of (a) weighting function and (b) head response for weighting function approximation using 3 and 10 exponential terms

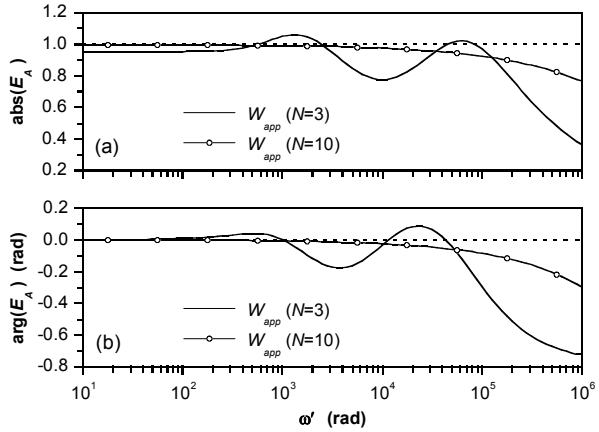

Figure 3. Behaviour of weighting function approximation error: (a) magnitude and (b) phase errors

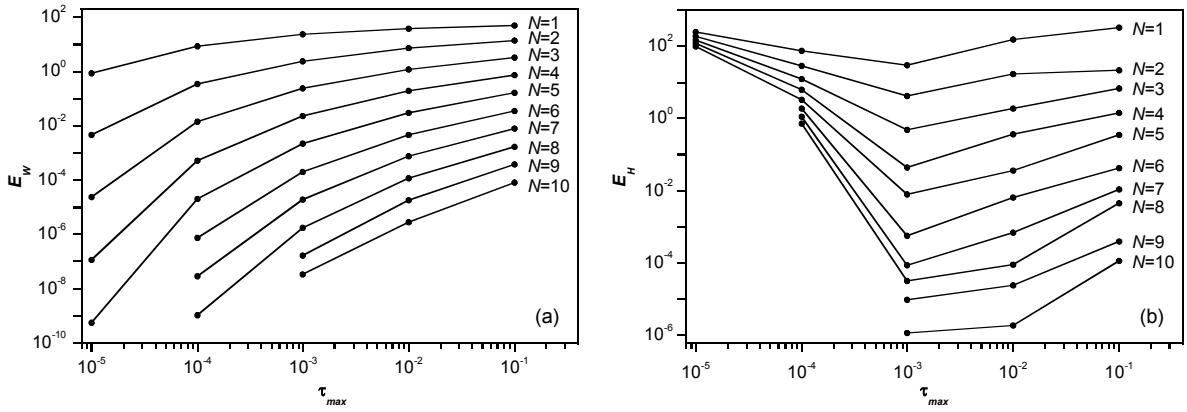

Figure 4. Trade-off curves between accuracy and efficiency: (a) relative weighting function error and (b) standardised head response error

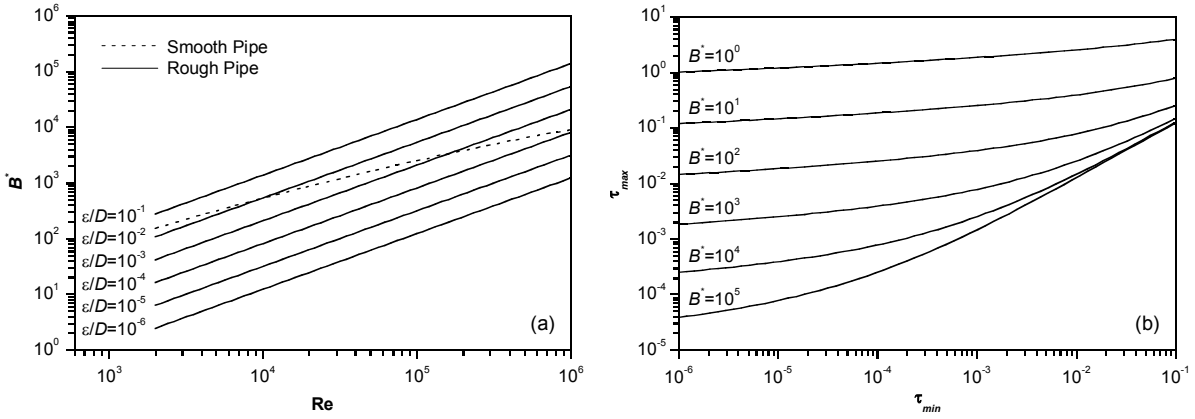

Figure 5. Investigation of variation of (a) B^* with Re and ε/D, and (b) τ range (= τ_{max} – τ_{min}) with B^*

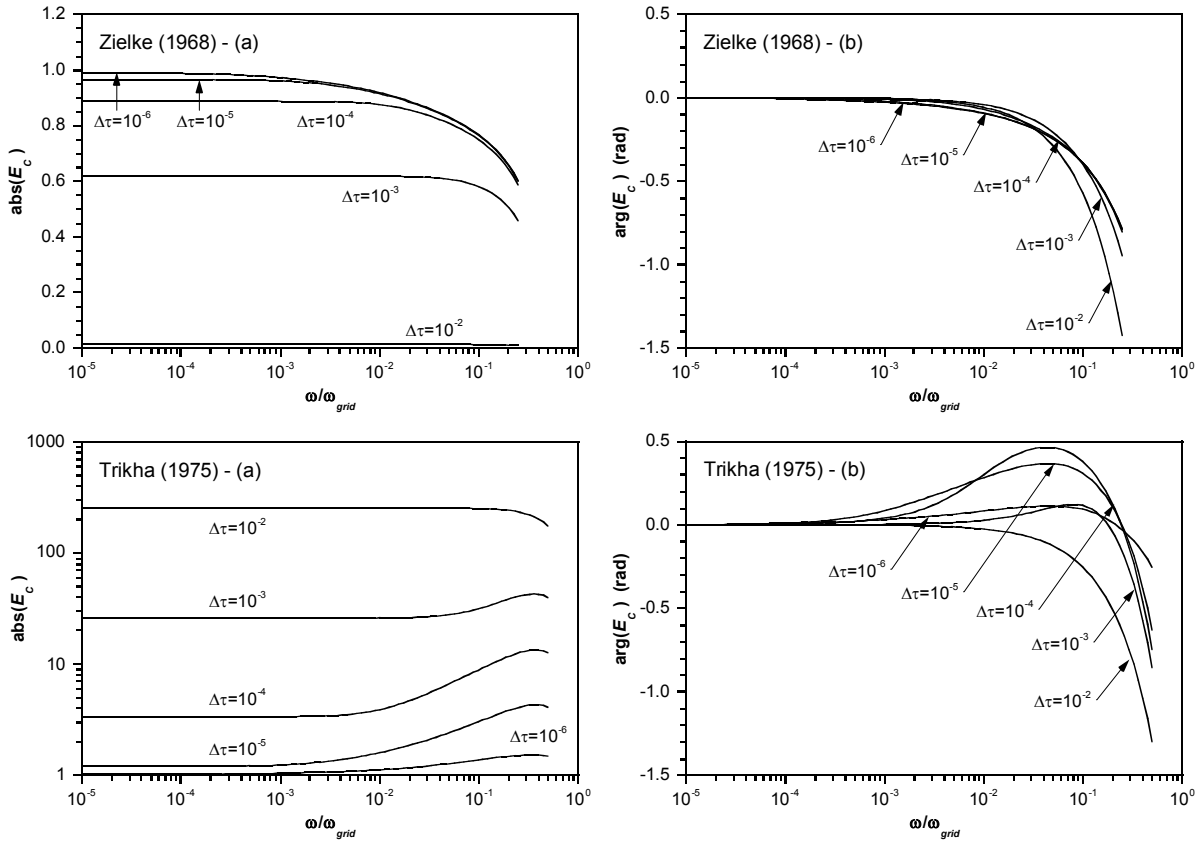

Figure 6. Convolution approximation error: (a) magnitude and (b) phase errors

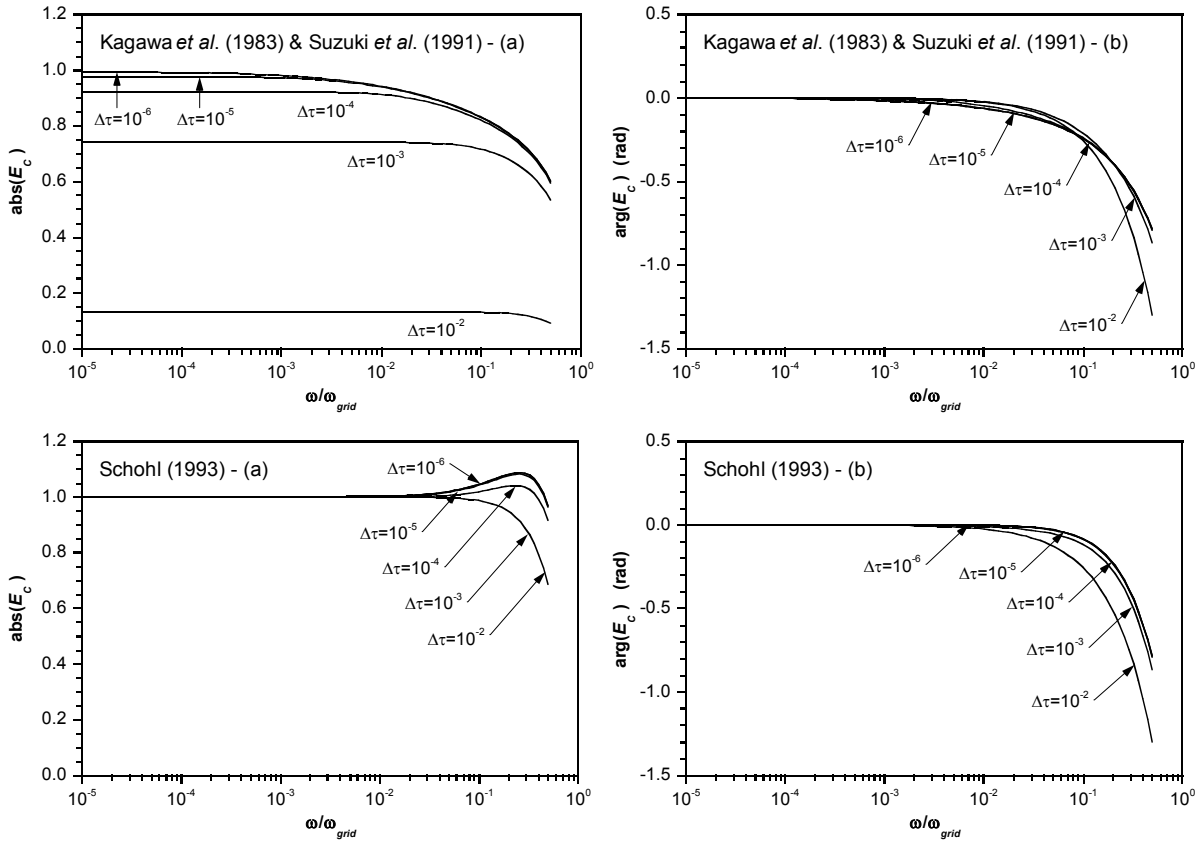

Figure 6(continued). Convolution approximation error: (a) magnitude and (b) phase errors

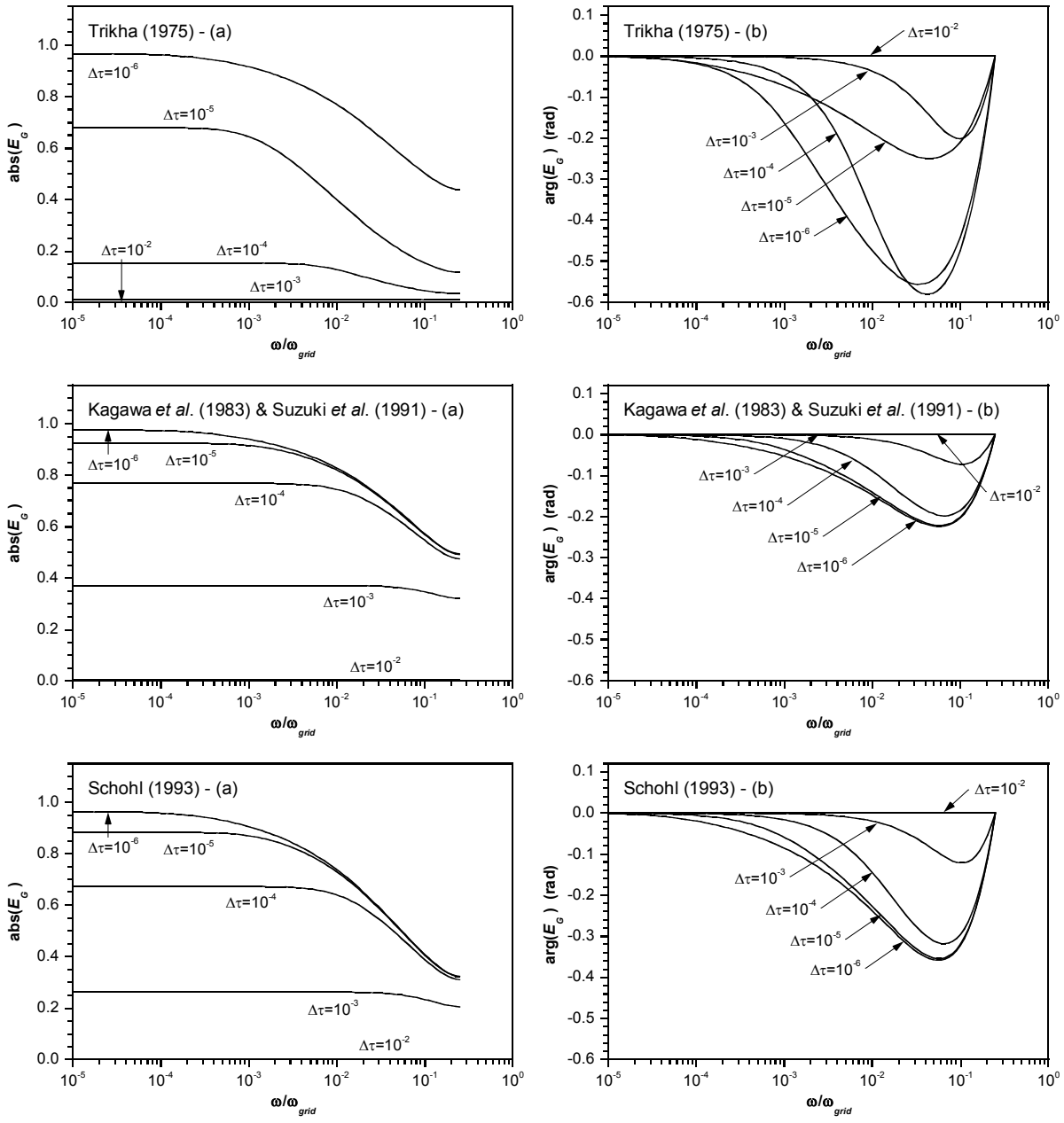

Figure 7. Grid separation error: (a) magnitude and (b) phase errors

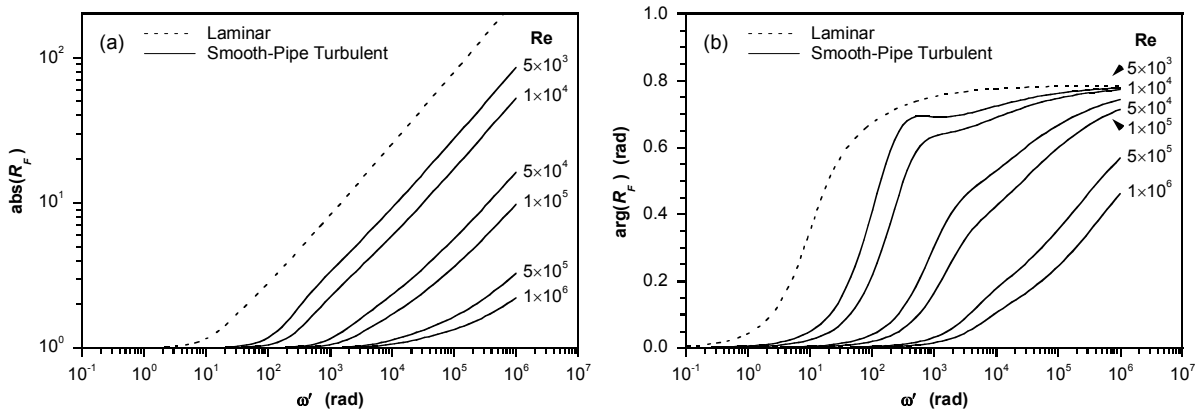

Figure 8. Behaviour of total unsteady/steady friction ratio: (a) attenuation ratio and (b) phase difference

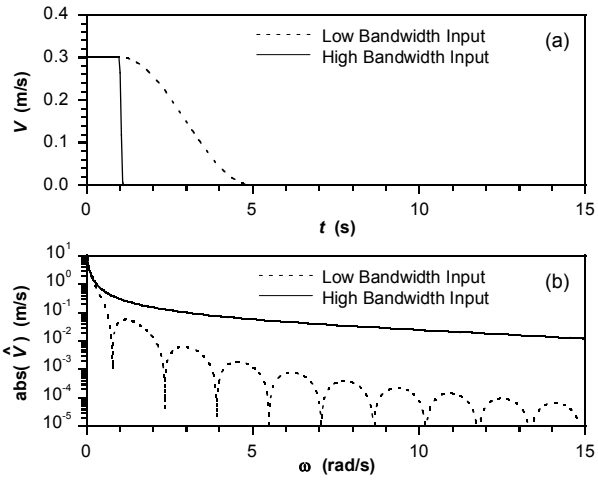

Figure 9. Input for limited input bandwidth example: (a) time domain and (b) frequency domain

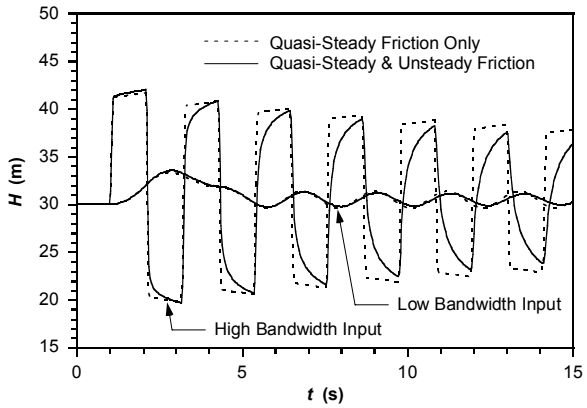

Figure 10. Time domain simulation for limited input bandwidth example

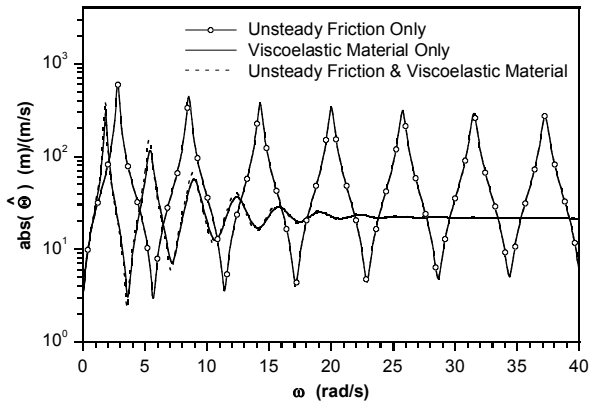

Figure 11. System transfer functions for limited system bandwidth and system component dominance example

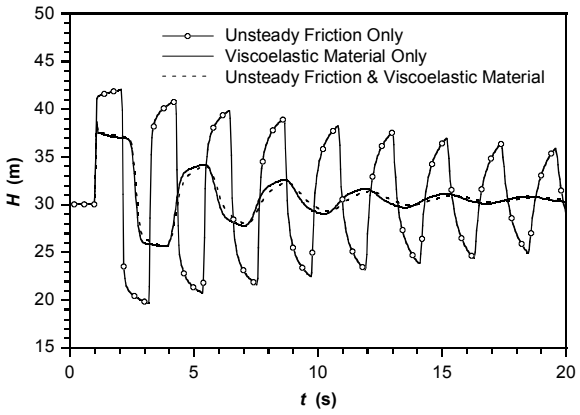

Figure 12. Time domain simulation for limited system bandwidth and system component dominance example